Deformation Behavior of Auxetic Woven Fabric Made of Foldable Geometry in Different Tensile Directions

Hasan Kamrul, Adeel Zulifqar, Shuaiquan Zhao, Minglonghai Zhang and Hong Hu*
Institute of Textile and Clothing, The Hong Kong Polytechnic University, Hung Hom, Hong Kong
*The corresponding author: hu.hong@polyu.edu.hk

Abstract

Auxetic woven fabrics made with special geometrical structures have gained the interest of textile scientists in recent years. This paper reports a study on auxetic woven fabric based on a double directional parallel in-phase zig-zag foldable geometrical structure. Such a fabric has been already produced and investigated for its negative Poisson's ratio effect in two principal directions (weft and warp direction). However, its negative Poisson's ratio effect in biased tensile directions as well as under repeated tensile loading conditions has not been studied yet. Therefore, in this paper, these two limitations are addressed. The auxetic woven fabric was firstly fabricated, and then subjected not only to tensile tests in different tensile directions including two principle directions and three biased directions, but also to repeated tensile loading. It was found that both the negative Poisson's ratio effect and the resistance to tensile deformation are dependent upon the tensile direction, and the highest negative Poisson's ratio effect and higher resistance to tensile deformation are obtained in two principal directions.

Keywords: negative Poisson's ratio, woven fabric, geometrical structure, deformation behavior, and resistance to tensile deformation, different tensile directions.

1. Introduction

Over the past few years, many studies have been conducted to investigate auxetic effect or negative Poisson's ratio (NPR) effect of different textile materials including auxetic fibers[1,2], auxetic yarns[3-5], auxetic knitted fabrics [6-9], auxetic woven fabrics[10-13], auxetic braided structures[14, 15], auxetic non-woven and auxetic textile composites[16-18]. Compared to conventional fabrics, auxetic fabrics exhibit NPR, which equips them with a number of unconventional properties. These include synclastic behavior under bending condition[19], better shape fitting ability, and reduced garment pressure exerted by the fabric on joint parts of the human body during movement or exercise[20-26]. Another important property is pores opening behavior under tension, which leads to increased air permeability of fabrics and controlled drug delivery for wound healing[10, 27, 28]. In addition, other properties including sound absorption[25], energy absorption ability[26,] and vibration damping[29, 30]could be improved. These properties make auxetic fabrics a very attractive choice for many applications such as protective sportswear[31], children's wear for size adaptability[8], functional underwear[32], medical applications[33], blast curtain[34], maternity clothes[9], aerospace, and military applications[32].

Auxetic fabrics can be fabricated using auxetic or non-auxetic yarns[35, 36]. To date, auxetic fabrics produced using auxetic yarns and weaving technology have helical auxetic yarns (HAYs) as weft yarns or warp yarns[5, 27, 37]. When HAYs were used as weft yarns, it was found that the auxetic fabrics made with plain and twill weave showed a better NPR effect than the fabric made with satin weave[10]. Recently, auxetic plied yarns were also used to fabricate auxetic woven fabrics, and it was found that the alternative arrangement of S- and Z-twisted auxetic plied yarns in a woven fabric can produce a higher NPR effect[38]. It should be noted that the use of auxetic yarns to fabricate auxetic fabrics makes the weaving process very complicated as auxetic yarns have to

be precisely arranged in woven structure to get the NPR effect. In addition, the NPR effect of auxetic yarns cannot be completely transferred to the woven fabric, because of the obstructions rendered by the interlacement points in the woven fabric structure. Therefore, using non-auxetic yarns to fabricate auxetic woven fabric has become a most used way. In this method, the key technique is to realize an auxetic geometry into fabric structure. Adopting this technique, various auxetic fabrics have been developed by using both knitting and weaving technology. Liu et al. produced auxetic weft knitted fabrics based on a Miura-origami structure by using flat knitting[7]. Hu et al. designed and fabricated different types of auxetic weft knitted fabrics based on foldable structures, rotating rectangles, and reentrant hexagons[6]. In addition to auxetic weft knitted fabrics, auxetic warp knitted fabrics were also fabricated based on the reentrant hexagonal geometry[39], rotational hexagonal loops geometry[40], double arrowhead geometry[41], and spacer structure8. However, these auxetic knitted fabrics have some limitations, such as higher thickness and low structural stability, which confined their applications in certain areas.

On the other hand, different types of auxetic woven fabrics were also produced based on foldable geometry[11, 42], rotating rectangle geometry[13], and reentrant hexagonal geometry (REHG)[43] through the creation of differential shrinkage or non-uniform contraction profile within the unit cells of the fabric structure. This was achieved by using elastic and non-elastic yarns, as well as combinations of loose and tight weaves. It was reported that these auxetic woven fabrics have NPR effect over a large range of tensile strain when stretched in either principle direction (warp and weft directions)[11, 42, 43], and if used in real life applications such as sportswear, they can improve the shape fitting ability at joint parts. In such applications, the NPR effect of fabrics in different tensile directions becomes important, because they are stretched repeatedly not only

in principle directions but also undergo repeated stretching in biased directions during real-life usage[12, 35, 44]. However, most of the researches on auxetic woven fabrics are still limited to the NPR effect in two principle directions under one stretch condition. Although a study is reported on the NPR effect and resistance to tensile deformation under repeating tensile cycles (RTCs) in different tensile directions for REHG woven fabric[12], similar research for other auxetic woven fabrics cannot be found in the literature.

This paper presents a study on the NPR effect and resistance to tensile deformation under RTCs in different tensile directions for auxetic woven fabric made with foldable geometry. Such a fabric has been already produced and investigated for its negative Poisson's ratio effect in two principal directions (weft and warp directions)[11]. It is expected this new study can further provide more useful information that can be adopted in the design of such type of fabrics for real-life applications.

2. Experimental

2.1 Fabrication of auxetic woven fabric

It is reported that the NPR effect can be induced into a woven fabric structure by adopting special interlacement patterns based on special auxetic geometrical structures[6, 12]. Those interlacement patterns consist of an array of unit cells that possess differential shrinkage effects at different sections of fabric. Therefore, upon relaxation, the different shrinkage behavior at different parts of the unit cell leads to the realization of the auxetic geometrical structure into the fabric. Using this approach, Cao et al. fabricated auxetic woven fabric based on an auxetic geometry as shown in Figure 1(a)[11]. Figure 1(b) shows the minimal repeating unit of this foldable structure.

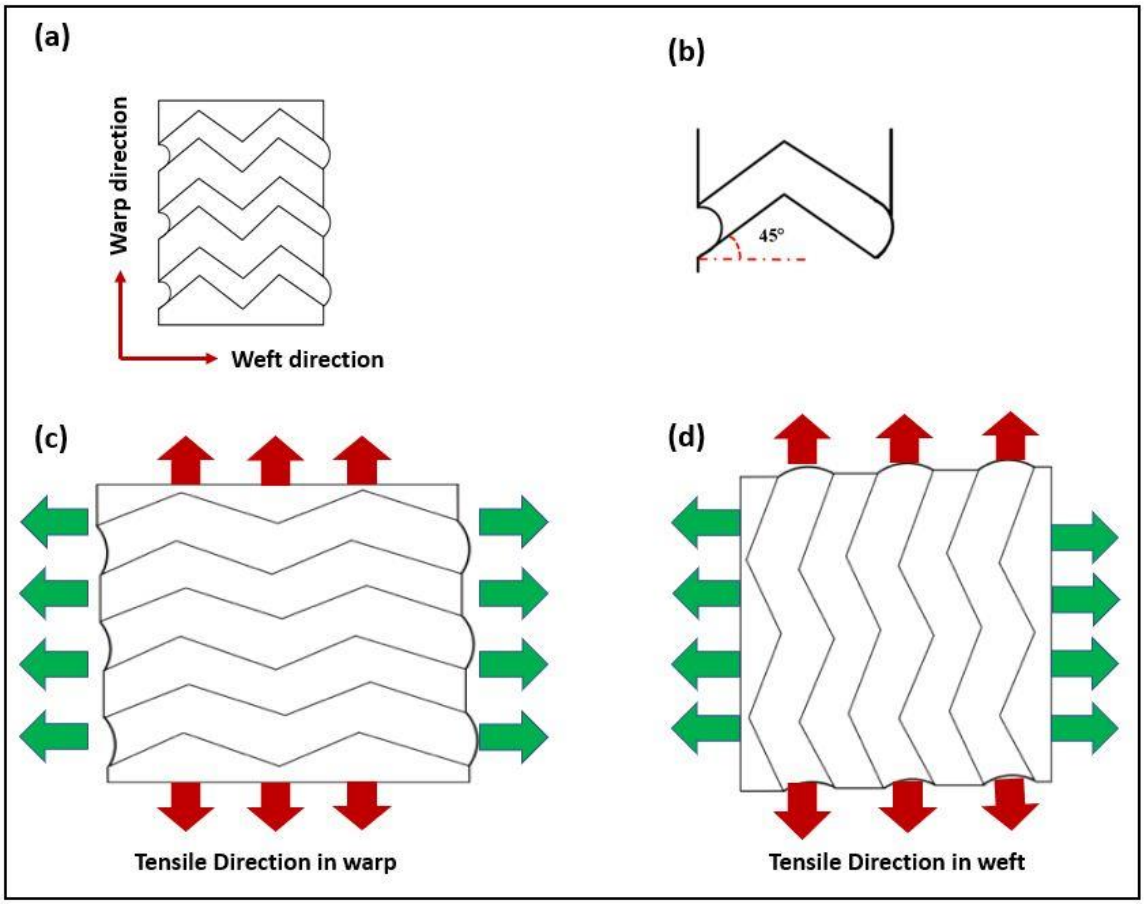

Figure 1. Auxetic geometry based on double-directional folded strips in parallel in-phase zig-zag fashion: (a) relaxed state; (b) unit cell; (c) stretched along the warp direction; (d) stretched along the weft direction.

This structure has alternate double-directional in-phase parallel zigzag foldable and flat stripes running along the weft direction with a connecting angle of 45°, which allows the design of symmetric interlacement pattern. Upon stretching in any direction, this foldable structure can be unfolded increasing the dimensions in the lateral direction, thus producing the NPR effect as shown in Figure 1(c) and (d), respectively.

In this study, the auxetic woven fabric was designed and fabricated using the same geometry and yarn materials. As shown in Figure 2 (a), the repeating unit of the interlacement pattern was designed based on a combination of alternative loose and tight weave stripes. The loose and tight weaves were placed in a manner that they made parallel in-phase zig-zag stripes running along the weft direction. The plain weave (1/1) was used as a tight weave and twill weave (3/1) with a floating length of 3 was used as a loose weave. It was observed that when the fabric was in a relaxed state, the twill weave (3/1) created a loose weave effect with higher shrinkage into the unit cell. Conversely, the plain weave (1/1) created a tight weave effect with lower shrinkage into the unit cell. Therefore, the higher shrinkage of the loose weave area forced the tight weave area to collapse and create double-directional folds in a parallel in-phase zig-zag fashion, which can be unfolded upon stretch to achieve an NPR effect. It was also observed that longer floats, which are formed because of the joining of long floats of adjacent yarns at the middle and edges of the unit cell, might influence the stability of the fabric structure. Therefore, the warp yarns at positions '0' were lowered to break these too long floats in the weft direction as shown in Figure 2(a). The fabric was fabricated by using all elastic yarn in the weft direction and alternate elastic and non-elastic yarn arrangement in the warp direction with the proportion of half elastic and half non-elastic yarn. This alternate elastic and non-elastic yarn arrangement was used because it was observed that the elastic yarns generate elasticity into the fabric structure and act as a return spring, while the non-elastic yarns make the fabric unit cell more stable. In addition, because of the different tensile properties of two types of yarns, differential shrinkage effect was created within the fabric unit cell. Since the combination of alternative elastic and non-elastic yarns was used in the warp direction, a rapier weaving machine (Model: SL8900S) manufactured

by CCI Intech with separate control systems for both beams was used. Furthermore, the warp yarns were sized by water-soluble polyvinyl alcohol (PVA), which can be de-sized after normal washing. The details of the yarns used are listed in Table 1.

Table 1. Details of the yarns used

Type of yarn	Structure of yarn	TPI of yarn	Linear density (Tex)
Non-elastic yarn	Cotton spun yarn	24.32	14.8
Elastic yarn	Core-spun cotton spandex yarn with a 40-denier spandex filament	26.61	14.8

After weaving, the fabric was subjected to relaxation for 48 hours at standard atmospheric conditions (25±2^{o}C and 65±2 RH). The fabric was then washed for 45 minutes in a Whirlpool washing machine (model: 3LWTW4840YW) followed by drying and relaxation at room temperature for 24 hours. After relaxation, the differential shrinkage effect was created into the fabric structure and double-directional folds in a pre-designed parallel in-phase zig-zag manner were formed, which can be unfolded upon stretch to achieve an NPR effect. Figure 2(b) shows the produced auxetic woven fabric, and the details of the fabric, including yarn arrangements and the drawing in the draft (repeat of warp yarn filling pattern into the healed frames), are given in Table 2.

Table 2. Details of the auxetic fabric structure based on foldable geometry

Warp density (/cm)	Weft density (/cm)	Tight weave	Loose weave
26. 40	24.20	Plain weave (1/1)	Twill weave (3/1)
Drawing-in draft	Frame No. 1 2 3 4 5 6 7 8 9 10 11 12 13 14 15 16 17 16 15 14 13 12 11 10 9 8 7 6 5 4 3 2 Yarn No. 1 2 3 4 5 6 7 8 9 10 11 12 13 14 15 16 17 18 19 20 21 22 23 24 25 26 27 28 29 30 31 32		

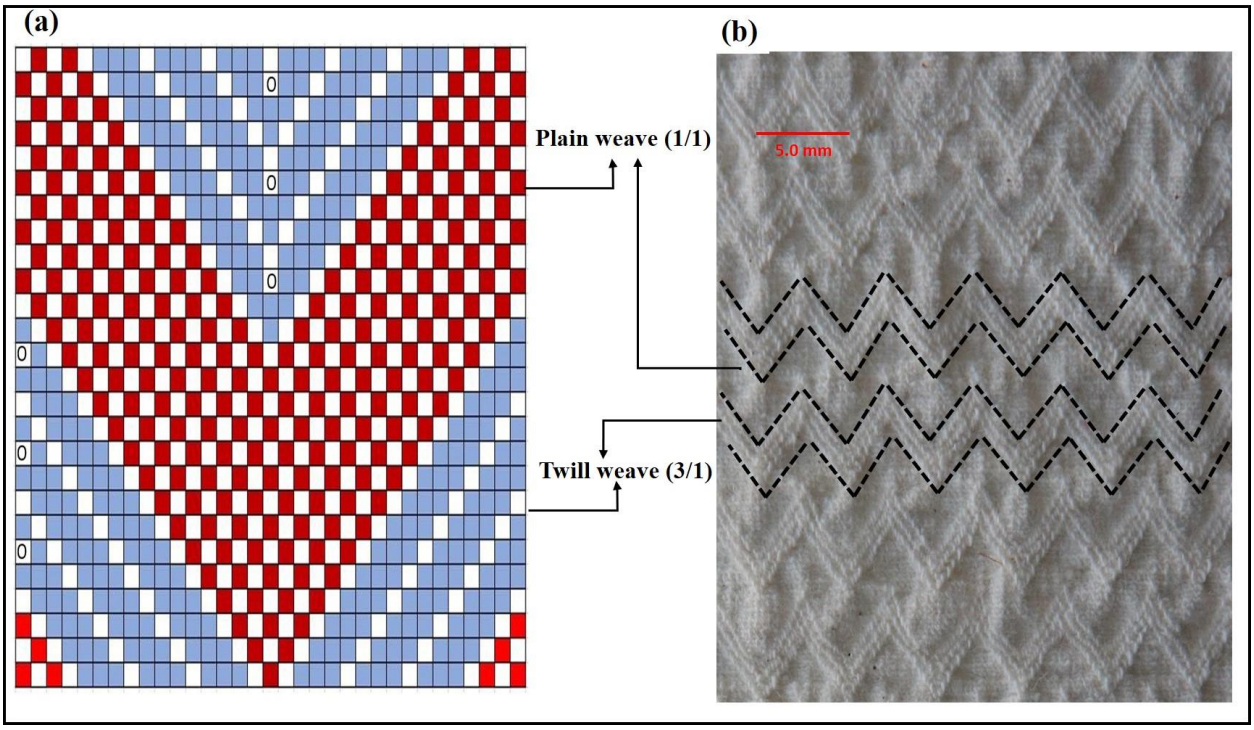

Figure 2. Auxetic woven fabric based on foldable geometry: (a) schematic illustration of arrangements of plain (1/1) weave and twill weave (3/1) within the unit cell of the interlacement pattern; (b) fabric at relaxed state showing outlines of unit cells.

The realization of folds in the fabric can be observed in Figure 2. After relaxation, the yarns within the unit cell at loose weave areas tend to be closed due to more shrinkage of elastic yarns than non-elastic yarns. At tight weave areas with small floats of warp and weft yarns, the yarns are firmly woven and are not as mobile as in loose weave areas. Consequently, tight weave areas undergo lesser shrinkage as compared to the loose weave areas, creating the differential shrinkage within the fabric structure. The higher shrinkage of the loose weave areas will force

the tight weave areas to collapse and create double-directional folds in a parallel in-phase zig-zag fashion.

2.2 Testing

To measure the NPR effect in five different tensile directions, the specimens of the auxetic woven fabric were subjected to the tensile test. The tensile directions included two principal directions and three biased directions. Figure 3 shows the schematic illustration of specimens in these tensile directions. The photos of test specimens showing the outlines of the unit cell in different tensile directions are presented in Figure 4. A square was marked on each specimen to facilitate the measurement of the size changes in both tensile and transverse directions during the tensile tests, as shown in Figure 5(a).

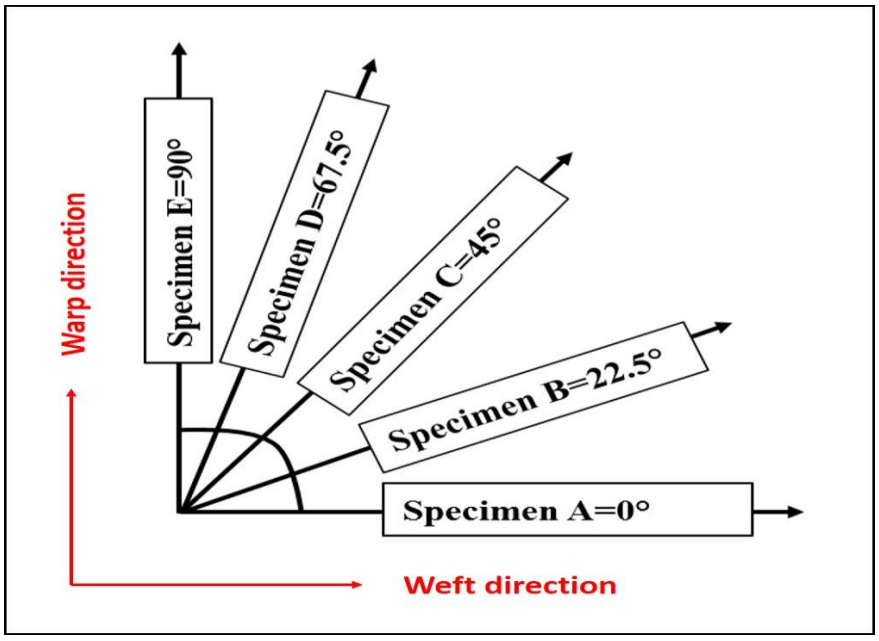

Figure 3. Schematic illustration of the testing specimen in different tensile directions.

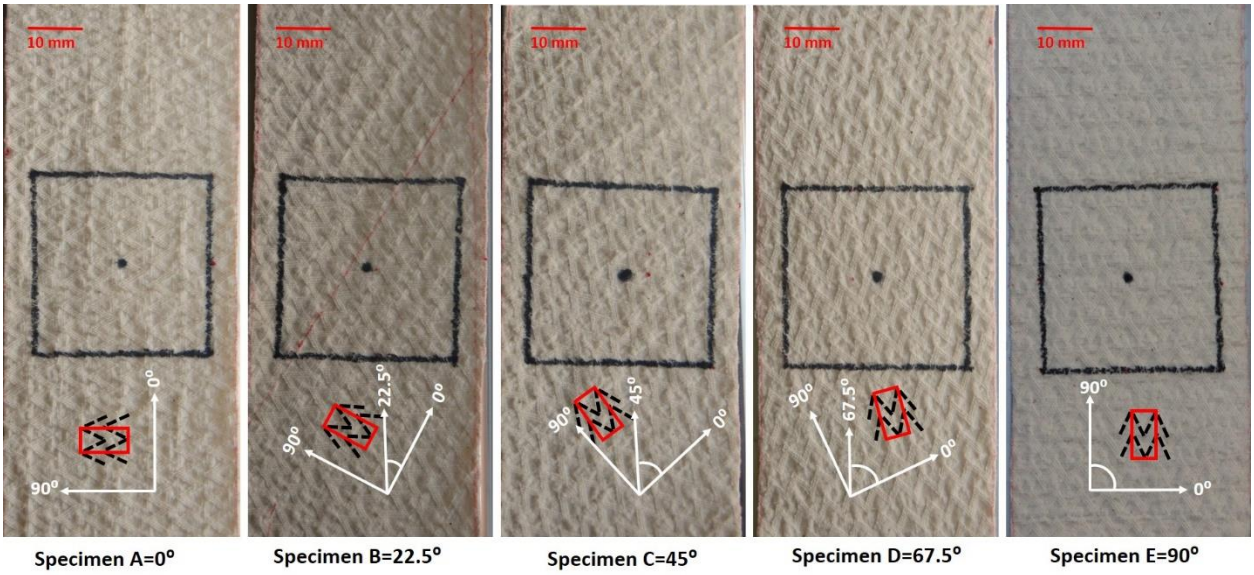

Figure 4. Photos of the testing specimens showing the orientation of unit cell in different tensile directions.

ASTM D5035-95 standard was followed and Instron 5566 tensile testing machine was used to conduct the tensile test with the following parameters: gauge length (150 mm); crosshead speed (50 mm/min); pre-tension (0.2 N); and sample size (200 mm ×50 mm). Three specimens were used for testing in each tensile direction with the same parameters until the breaking of fabric. To measure the size change in tensile and transverse directions, the tensile process was video-recorded by a high-resolution camera (Canon-EOS 80D) which was placed on a tripod in front of the specimen, as shown in Figure 5(b). Then the photos were extracted from the video with an interval of 2–3 seconds or 1% of tensile strain. A photo was also taken before the start of tensile testing, which was considered as a photo of the specimen in the un-stretched state. This photo was used to make a comparison with photos of the fabric extracted from the video at different tensile strains. In the photos, the distances between the line marks in the tensile and transverse directions were measured via a screen ruler for both un-stretched and the stretched states at

different tensile strains of each specimen. After that, the engineering strains of the fabric structure were calculated in both the transversal and tensile directions through Eqs. (1) and (2).

$$\varepsilon_y = \frac{Y - Y_0}{Y_0} \quad (1)$$

$$\varepsilon_x = \frac{X - X_0}{X_0} \quad (2)$$

Where ε_y is the transversal strain, ε_x is the tensile strain, Y and Y_0 are the initial and extended length in the transversal direction, respectively, X and X_0 are the initial and extended length in the tensile direction, respectively. Finally, Poisson's ration v was calculated via Eq. (3).

$$v = -\frac{\varepsilon_y}{\varepsilon_x} \quad (3)$$

It is important to mention that the stress-strain curves were generated automatically by the Instron 5566 tensile testing machine.

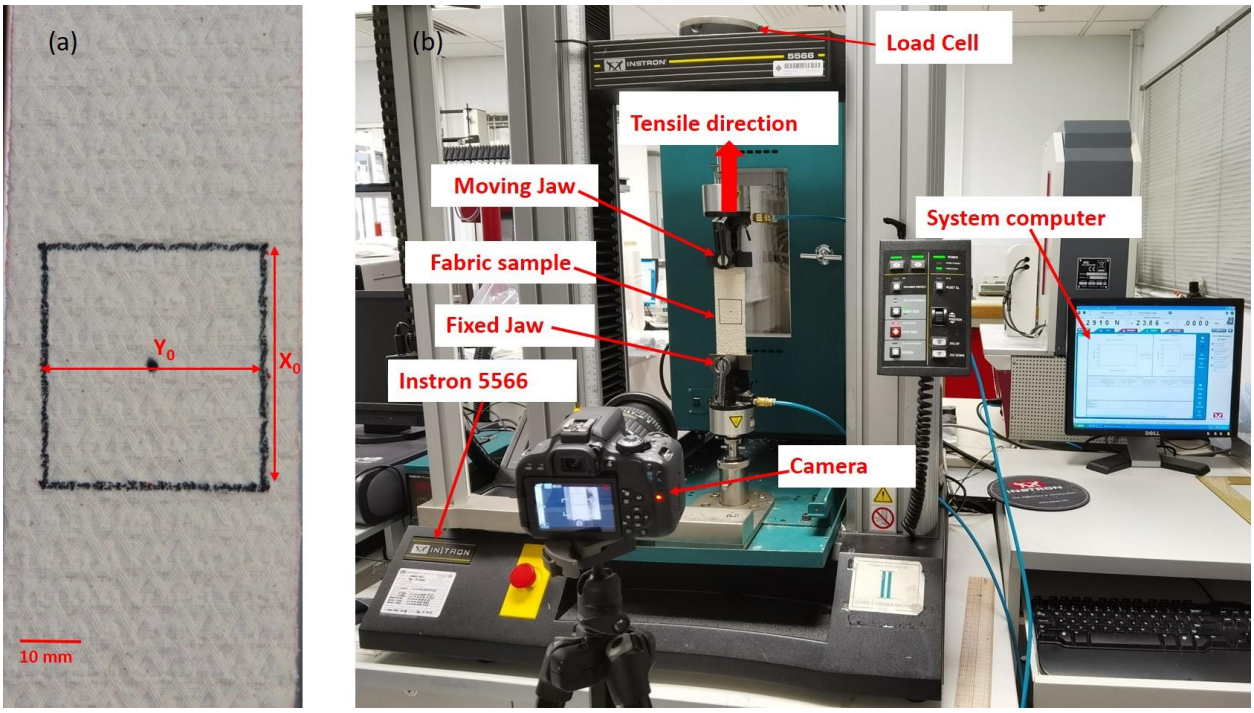

Figure 5. Tensile testing setup: (a) fabric specimen; (b) photo of the specimen, Instron 5566, and camera.

The RTCs test was also conducted to study the variation in the NPR effect after repeated tensile loading and resistance to tensile deformation. It is highlighted that the same tensile testing setup as shown in Figure 5(b) and parameters were used for the RTCs test. Figure 6 systematically illustrates the RTCs test process at the different tensile strain. Each specimen was tested for 20 RTCs. During each tensile cycle, the fabric specimen was stretched up to 25% of the tensile strain, then it was kept there for 10 seconds, and after that, it was returned to its original position at the same speed and kept there again for 10 seconds for relaxation. This process for the individual tensile cycle was repeated until the completion of 20 cycles for each specimen. The video of the entire process of the RTCs test was also recorded and the Poisson's ratio was calculated following the same method as explained above. Three specimens were used for testing in each tensile

direction and average Poisson's ratio values at tensile strains of 5%, 10%, 15%, 20%, and 25% were calculated for each tensile cycle. Finally, the Poisson's ratio for each tensile direction was plotted against the number of tensile cycles to study the influence of RTCs test on the NPR effect of the fabric and the resistance to tensile deformation in each tensile direction.

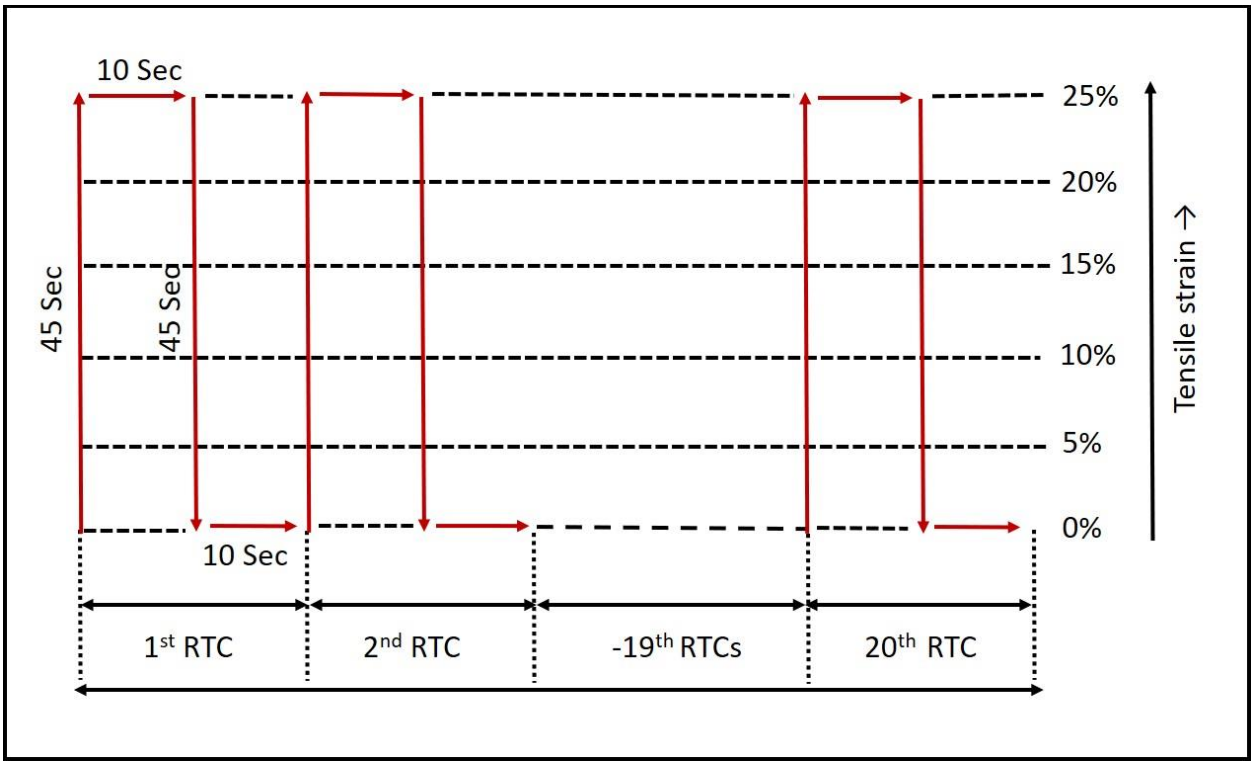

Figure 6. Schematic illustration of the RTCs test.

3. Results and discussion

3.1 Auxetic behavior at different tensile directions

Upon stretch, the double-directional folds are unfolded, and the transverse dimension is increased, therefore, the NPR effect is achieved. Figure 7 compares Poisson's ratio versus tensile strain curves for the auxetic woven fabric when the fabric specimens are stretched in different

tensile directions. It can be observed that every specimen has an NPR effect over a different range of tensile strain and the highest NPR effect is achieved along the two principal directions compared to the three biased directions. Specifically, the highest NPR values of -0.36 and -0.24 are obtained at the tensile strain of 2-5% along the warp and weft directions, respectively. Upon further stretching in the warp direction, the NPR sharply decreases and reaches up to -0.16 with the increase of tensile strain to 12%. After that, the NPR gradually decreases with increasing tensile strain and becomes zero at 67% tensile strain. When the specimen is stretched in the weft direction, the NPR effect rapidly decreases, and the NPR value reaches -0.10 at 12% tensile strain. Afterward, the NPR starts to gradually decrease up to the tensile strain of 24% and keeps stable up to 48% tensile strain. After that, the NPR value again decreases with the increase of tensile strain. It is observed that the fabric keeps the NPR effect even when the tensile strain reaches 90%. These results indicate that the fabric has the NPR effect over a large range of tensile strain in both principal directions. In addition, the NPR effect is also achieved when the fabric is stretched along biased directions as shown in Figure 7. However, the NPR effect is obtained only over a smaller range of tensile strain. Furthermore, the NPR reaches the highest level at the initial stage of tensile strain, then gradually decreases to zero with the increase of tensile strain. Particularly, the highest NPR of –0.18 is obtained at a tensile strain of 3% when the fabric is stretched along the 22.5^{o} biased direction, and the lowest NPR effect is achieved when stretched along the 67.5^{o} biased direction. It is found that the NPR effect is kept only up to 14% tensile strain when the fabric is stretched along 45^{o} and 67.5^{o} biased directions. Besides, the NPR effect is kept up to a tensile strain of 18% when stretched along the 22.5^{o} biased direction.

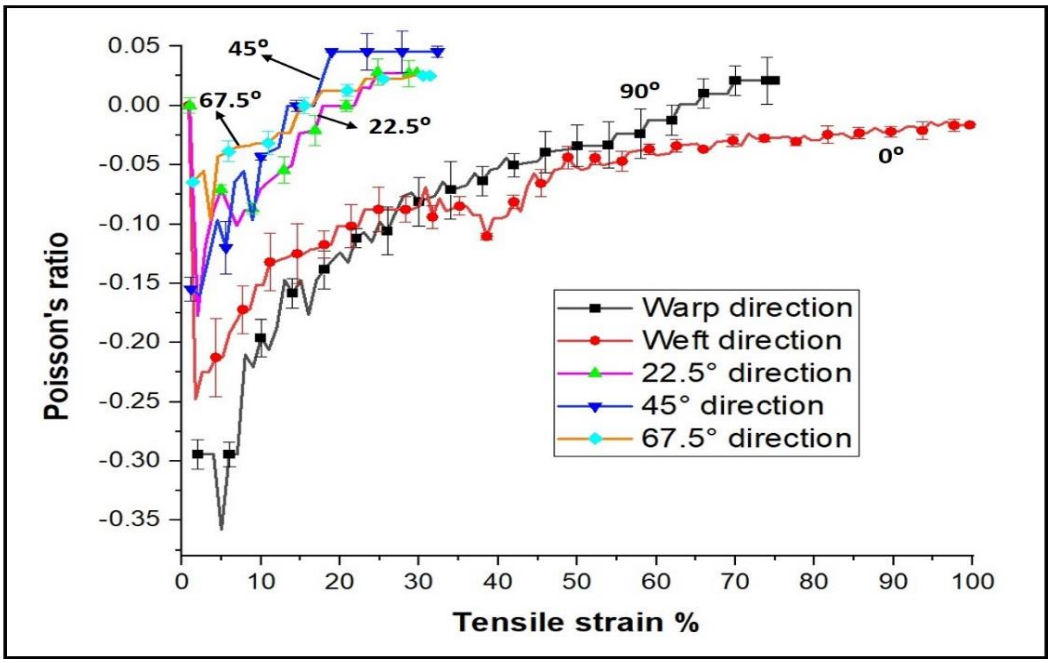

Figure 7. Poisson's ratio versus tensile strain curves in different tensile directions.

It was observed that in all tensile directions, the NPR effect significantly increases at the initial stages of the tensile strain and then decreases with the increase of the tensile strain. The reason for this behavior is that when the fabric is stretched in different tensile directions, the transposition of yarn shrinkage at the loose weave areas takes place due to more yarn mobility in these areas. The yarns in tensile direction then tend to get straight orientation to the tensile direction and the double directional folded area comes with an opening in the transverse direction immediately at the lower tensile strains. Therefore, a higher NPR is achieved at the initial stage of tensile strain. Upon further stretching, the yarns in tensile direction at loose weave areas continue to extend until the transposition of shrinkage at loose weave areas is completed. Therefore, the yarns in tensile direction then start moving apart to shift towards the position that they held at tight weave areas. This increases the values of tensile strain and starts to decrease

the value of the NPR. Subsequently, at higher tensile strains, the slippage effect at the cross over points of warp and weft is reached and the fabric undergoes contraction in the transverse direction, which results in positive Poisson's ratio. Besides, it was also observed that at higher tensile strains, the fabric experiences an out of plane angular deformation or buckling, which also leads to a contraction in the transverse direction, resulting in positive Poisson's ratio. However, there was no in-plane angular deformation observed across transverse direction throughout the tensile test. Furthermore, the NPR effect of the fabric is less when stretched along the weft direction as compared to the warp direction. This is because the shrinkage and folded effects are larger along the weft direction of the fabric and it can be observed clearly from Figure 8. Therefore, when the fabric is stretched along the weft direction as shown in Figure 8(a), because of the higher shrinkage and larger folded effect along this direction, the transposition of shrinkage at loose weave areas and the opening of the folded area along the warp direction occurs at higher tensile strain, which reduces the NPR value. On the other hand, when the fabric is stretched along the warp direction as shown in Figure 8(b), due to the smaller shrinkage and folded effect along this direction and larger folded effect along the weft direction, the transpose of shrinkage completes earlier and larger opening of the folded area along the weft direction is achieved even at smaller tensile strain, resulting in the higher NPR.

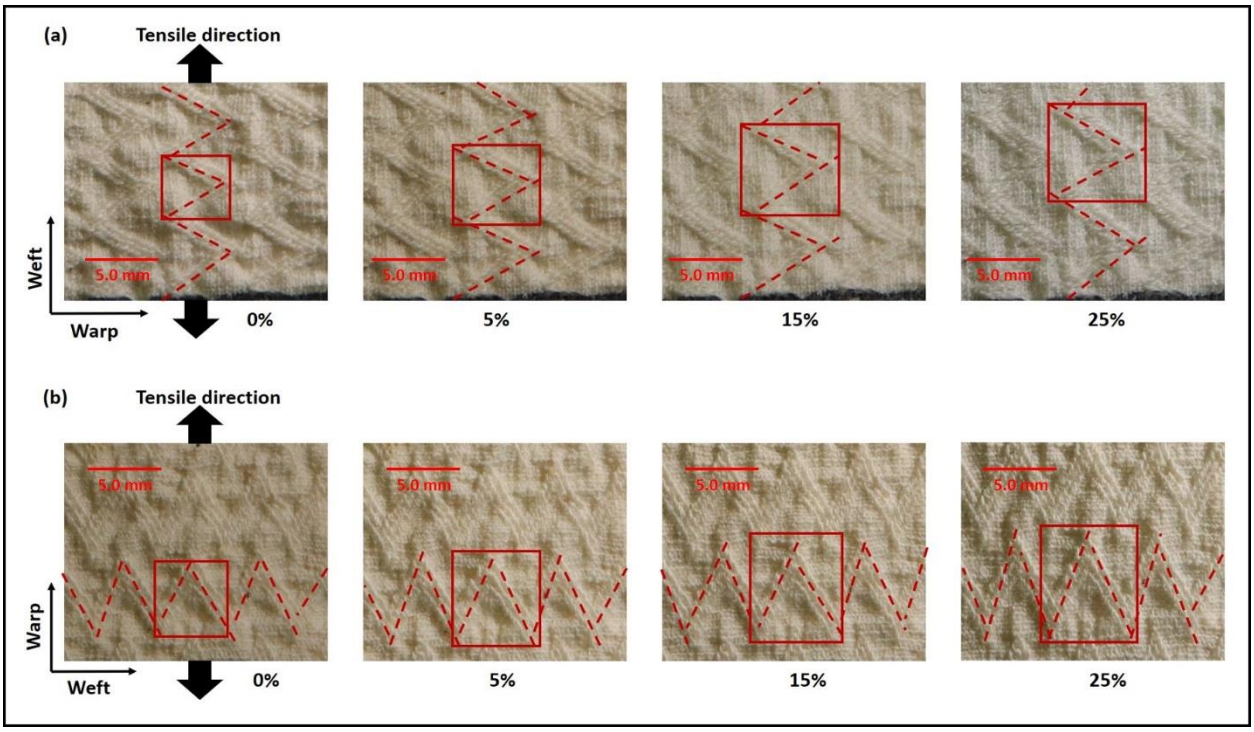

Figure 8. Photos of the fabric showing the deformation behavior of the unit cell at different tensile strains: (a) weft direction; (b) warp direction.

Furthermore, it can be observed from Figure 7, when the fabric is stretched along three biased directions, the NPR effect is almost similar at higher tensile strains. However, the NPR effect obtained at smaller tensile strains is larger when the fabric is stretched along the 22.5^{o} biased direction as compared to that produced when the fabric is stretched along with the 45^{o} and 67.7^{o} biased directions.

This might be because of the orientation of the unit cell. As shown in Figure 9, when the fabric is stretched in 22.5^{o} biased directions, the orientation of the unit cell is such that most of the folded section part of the unit cell experiences the stretching force, and larger opening of folded sections in the transverse direction is achieved which results in higher initial NPR. Furthermore, as the tensile strain increases in the case of all three biased directions, the unit cell loses its true

orientation which results in a contraction in transverse direction instead of expansion resulting in positive Poisson's ratio as shown in Figure 7.

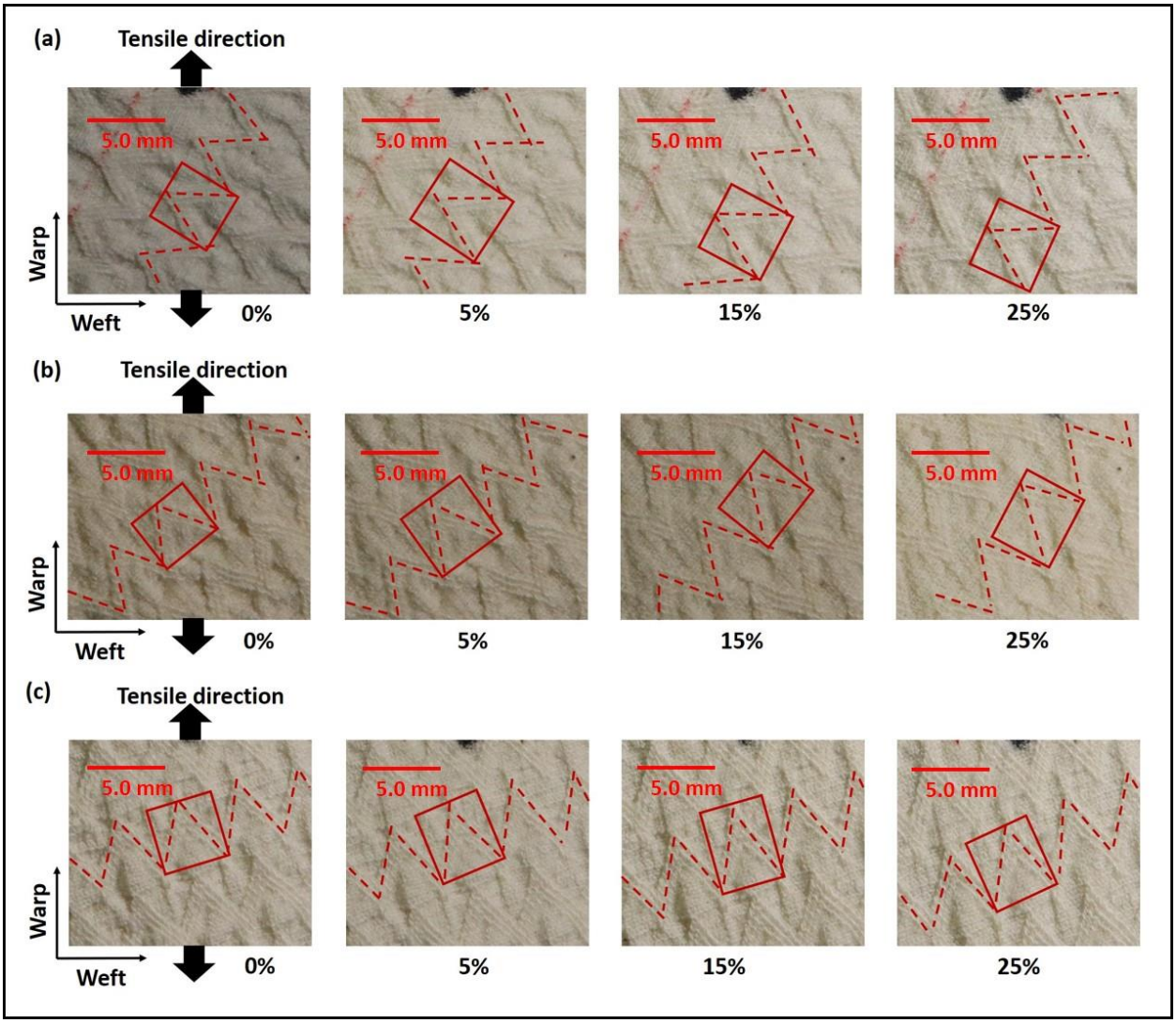

Figure 9. Photos of the fabric showing the deformation behavior of the unit cell at different tensile strains: (a) 22.5^{o} biased direction; (b) 45^{o} biased direction; (c) 67.5^{o} biased direction.

In addition to the orientation of the fabric structural unit cell, the NPR effect is also influenced by the fabric extensibility in different tensile directions. Figure 10 shows the tensile stress–tensile strain curves of the fabric in different tensile directions. When stretched in the biased directions,

the fabric has more extensibility as compared to the warp direction. In this case, the magnitude of tensile strain depends on the deviation of the tensile direction to the warp direction. This is because stretching the fabric in biased directions can result in three different conditions that are associated with warp yarns. Firstly, both ends of the warp yarns are clamped; secondly, only one end is clamped; and lastly, both ends of the yarn are free. Therefore, upon stretching in a biased direction that is further away from the warp direction, the existence of the second or third conditions becomes more obvious and the extensibility is increased. This means the direction of force application can produce the maximum elongation at a lower yarn tension. Because of this, the straightforward deformation of the foldable structural unit cell is lesser, and a smaller NPR effect is produced when the fabric is stretched in these biased directions.

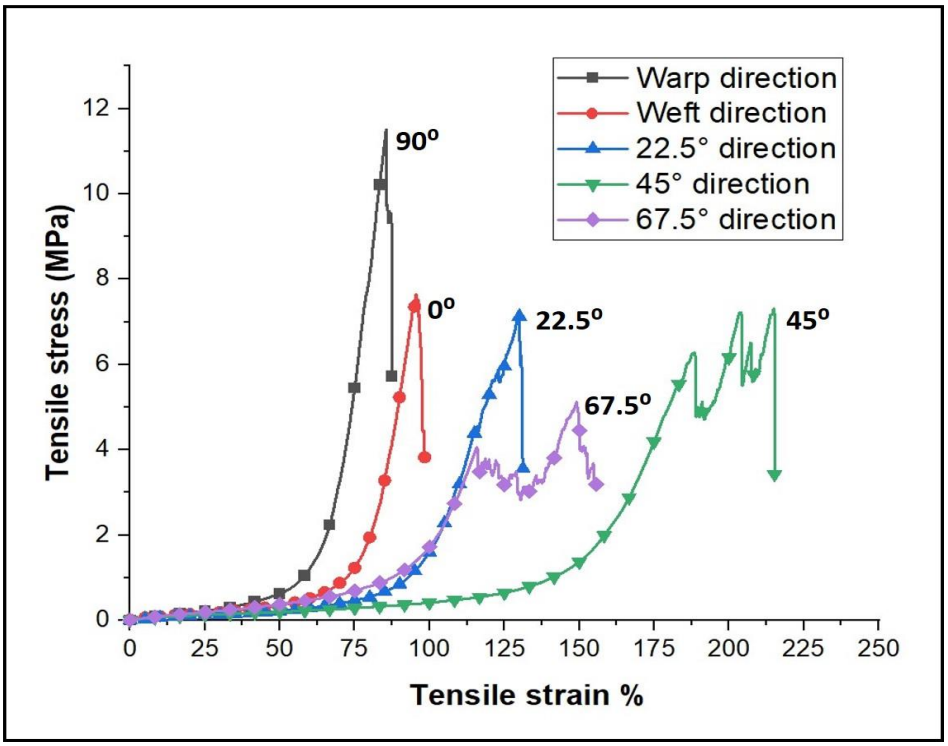

Figure 10. Tensile stress–tensile strain curves of the auxetic woven fabric in different tensile directions.

3.2 Auxetic behavior under repeated tensile cycles

Figure 11 shows the plots of Poisson's ratio as a function of tensile cycle at tensile strains of 5%, 10%, 15%, 20%, and 25%. It can be seen that for each stretch direction and at each level of tensile strain, the highest NPR effect is obtained after the first RTC at 5% of tensile strain and the NPR effect decreases with increasing RTCs. When the fabric is stretched in the warp direction, the highest NPR value of -0.36 is achieved at a tensile strain of 5% after the first RTC as shown in Figure 11(a). Afterward, the NPR effect is gradually decreased following every tensile cycle up to 6 RTCs, then the NPR effect is kept almost the same up to 20 RTCs. However, it is found that the fabric can keep around 70 % of the NPR effect after completing 20 RTCs for each level of tensile strain. Figure 11(e) shows the RTCs results in the weft direction where the highest NPR value of –0.26 is achieved at a tensile strain of 5% after the first RTC. It can be seen that the NPR value is decreased after every tensile cycle up to 11 RTCs, and then remains stable up to 20 RTCs. The fabric keeps around 60 % of the NPR effect after completing 20 RTCs.

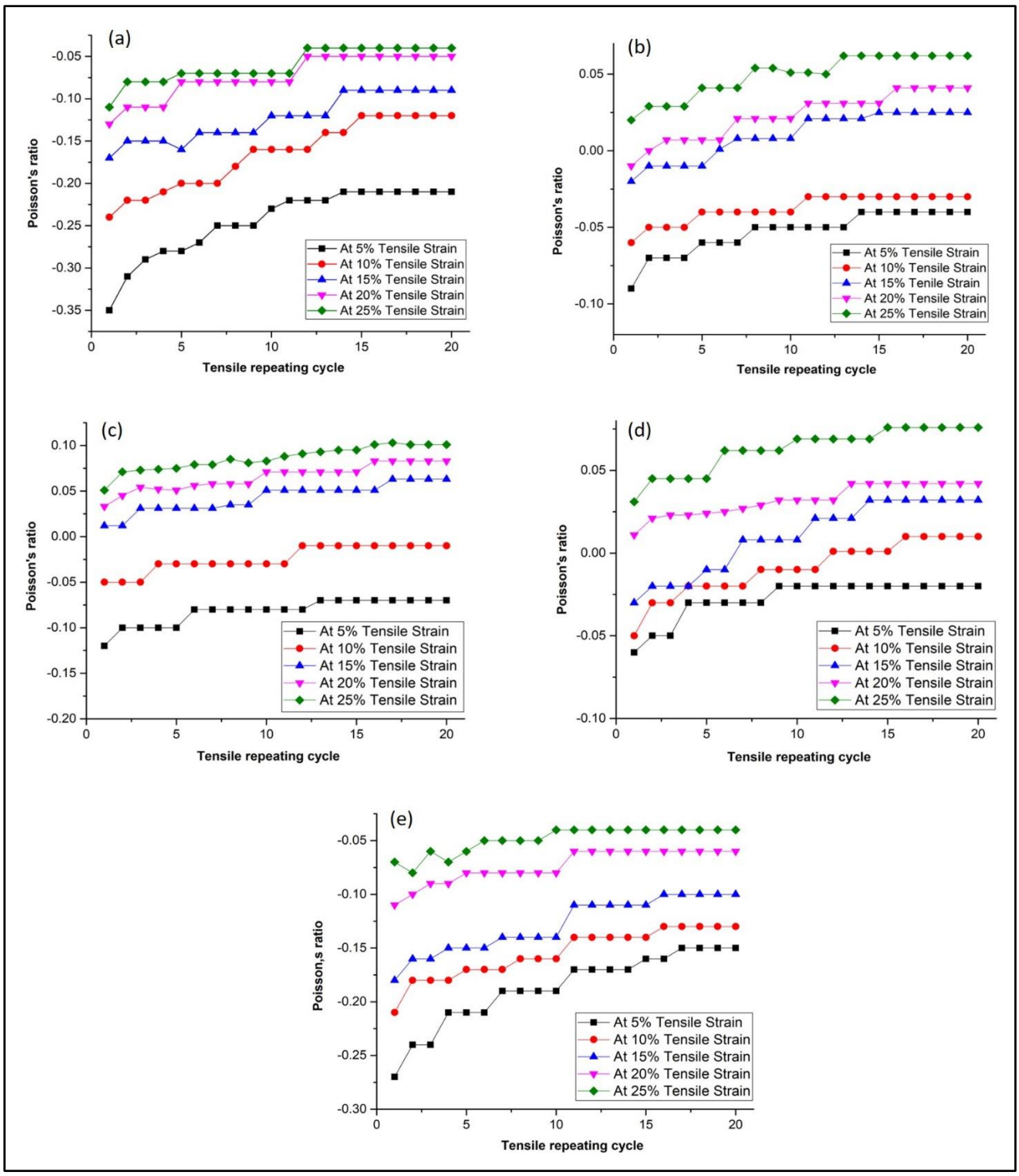

Figure 11. NPR effect under repeating tensile condition: (a) stretched in the warp direction (90^o); (b) stretched in the biased direction (22.5^o); (c) stretched in the biased direction (45^o); (d) stretched in the biased direction (67.5^o); (e) stretched in the weft direction (0^o).

Figure 11(b) shows Poisson's ratio versus tensile cycle plots when the fabric is stretched in 22.5^{o} biased direction at different tensile strains. It is observed that at tensile strains of 5%, 10%, and 15%, the fabric shows NPR effect at smaller RTCs which decreases with increasing RTCs and is lost at higher RTCs. It can also be observed that at the tensile strain of 5%, the highest NPR value of –0.12 is obtained and the NPR value is decreased with increasing RTCs until 5 RTCs and after that, the NPR value is kept the same up to 20 RTCs. Moreover, at 20% of tensile strain, the NPR effect is achieved at the beginning and no NPR effect is obtained after the second RTCs. Furthermore, at 25% of tensile strain, no NPR effect is achieved as shown in Figure 11(b). When the fabric is stretched in 45^{o} biased direction as shown in Figure 11(c), at 5% of tensile strain, the NPR effect is obtained which decreases with increasing RTCs until 13 RTCs, after that, the NPR value is kept the same until 20 RTCs. It is also observed that no NPR effect is obtained at 15%, 20%, and 25% of tensile strain. Finally, when the fabric is stretched in 67.5^{o} biased direction as shown in Figure 11(d), the highest NPR value of –0.07 is obtained at the tensile strain of 5%, and NPR is achieved even after completing 20 RTCs. Furthermore, at the tensile strain of 10% and 15%, only a smaller value of the NPR effect is achieved which is decreased with the increasing RTCs and is lost after 11 RTCs at 10 % of tensile strain and after 6 RTCs at 15% of tensile strain. However, at 20% and 25% of tensile strain, no NPR effect is obtained.

These results reveal that the NPR effect is influenced by the stretching direction and the number of RTCs. It is found that a higher NPR effect is produced when the fabric is stretched along the principal directions as compared to the biased directions. In addition, the resistance to the tensile deformation of the fabric is also higher in the principal directions as compared to the biased directions. Moreover, between two principal directions, the NPR effect and resistance to tensile

deformation along warp direction is higher than along weft direction. This is due to the fact that the unit cell is more stable along warp directions and can keep its shape even after completion of many RTCs. On the other hand, in case of biased directions, the fabric has higher extensibility along these directions, but the unit cell is not very stable and loses its shape easily. Therefore, the loss of the NPR effect is higher along these directions as compared to the principal directions. This means that the principal directions have a higher resistance to tensile deformation as compared to biased directions. Regarding the influence of the RTC, it is observed that the NPR effect is decreased with the increase of RTCs for each tensile direction. This might be because of the fact that there is a permanent deformation-induced into the fabric structure after every RTC. This result suggests it is very important to reduce the effect of repeated stretching on the NPR effect of fabrics, in other words, to improve the tensile deformation resistance ability. This can be achieved by the application of a finish or coating that has compatibility with the fabric in terms of flexibility, elongations, and other tensile properties.

Conclusions

This paper reports the development and analysis of bi-stretch auxetic woven fabric based on foldable geometry. The fabric was first fabricated by using non-auxetic yarns and combinations of loose and tight weaves. Tensile tests were conducted for five different tensile directions which include two principal directions and three biased directions. The tensile repeating test was also performed for each of the tensile direction to study the effect of repeated tensile loading on the NPR effect. The results have shown that fabric possesses auxetic behavior when stretched in all five directions. From this study, the following conclusions can be made.

1. Bi-stretch auxetic woven fabrics based on foldable geometry have the NPR effect in principal as well as in biased directions.

2. Higher NPR effect and tensile deformation resistance ability are obtained when the fabric is stretched in the principal directions as compared to those obtained in biased directions.
3. When the fabric is stretched in two principal directions, the higher NPR effect and tensile deformation resistance ability are obtained in the warp direction.
4. When the fabric is stretched in three biased directions, the highest initial NPR effect is obtained in 22.5^{o} biased direction at 5% of tensile strain.
5. No NPR effect is obtained at 20% and 25% of tensile strains when the fabric is stretched in 45^{o} and 67.5^{o} biased direction.
6. All three biased directions have larger extensibility as compared to the principal directions.
7. The NPR effect in each stretch direction decreases with increasing tensile cycles.
8. The developed auxetic woven fabric can keep around 60% of its NPR effect when stretched in the weft direction, but when it comes to the warp direction, it can keep 70% of its NPR effect after 20 repeating tensile cycles.

Acknowledgment

The authors would like to thank the funding support from the Research Grants Council of Hong Kong Special Administrative Region Government in a form of GRF project (grant number: 15209616)

References

1. Evans KE. Auxetic polymers: a new range of materials. *Endeavour* 1991; 15: 170-174.
2. Ravirala N, Alderson KL, Davies PJ, et al. Negative Poisson's ratio polyester fibers. *Textile research journal* 2006; 76: 540-546.
3. Ng WS and Hu H. Tensile and deformation behavior of auxetic plied yarns. *physica status solidi (b)* 2017; 254: 1600790.
4. Ge Z, Hu H and Liu S. A novel plied yarn structure with negative Poisson's ratio. *The Journal of The Textile Institute* 2016; 107: 578-588.
5. Sloan M, Wright J and Evans K. The helical auxetic yarn–a novel structure for composites and textiles; geometry, manufacture and mechanical properties. *Mechanics of Materials* 2011; 43: 476-486.

6. Hu H, Wang Z and Liu S. Development of auxetic fabrics using flat knitting technology. *Textile research journal* 2011; 81: 1493-1502.
7. Liu Y, Hu H, Lam JK, et al. Negative Poisson's ratio weft-knitted fabrics. *Textile Research Journal* 2010; 80: 856-863.
8. Wang Z and Hu H. 3 D auxetic warp-knitted spacer fabrics. *physica status solidi (b)* 2014; 251: 281-288.
9. Glazzard M and Breedon P. Weft-knitted auxetic textile design. *physica status solidi (b)* 2014; 251: 267-272.
10. Monika V and Petra V. Auxetic woven fabrics—pores' parameters observation. *Journal of Donghua University (English Edition)* 2013: 19.
11. Cao H, Zulifqar A, Hua T, et al. Bi-stretch auxetic woven fabrics based on foldable geometry. *Textile Research Journal* 2019; 89: 2694-2712.
12. Kamrul H, Zulifqar A and Hu H. Deformation behavior of auxetic woven fabric based on re-entrant hexagonal geometry in different tensile directions. *Textile Research Journal* 2019: 0040517519869391.
13. Zulifqar A, Hua T and Hu H. Development of uni-stretch woven fabrics with zero and negative Poisson's ratio. *Textile research journal* 2018; 88: 2076-2092.
14. Jiang N and Hu H. A study of tubular braided structure with negative Poisson's ratio behavior. *Textile Research Journal* 2018; 88: 2810-2824.
15. Rawal A, Saraswat H and Sibal A. Tensile response of braided structures: a review. *Textile Research Journal* 2015; 85: 2083-2096.
16. Imbalzano G, Tran P, Ngo TD, et al. A numerical study of auxetic composite panels under blast loadings. *Composite Structures* 2016; 135: 339-352.
17. Jiang L, Gu B and Hu H. Auxetic composite made with multilayer orthogonal structural reinforcement. *Composite Structures* 2016; 135: 23-29.
18. Yang S, Chalivendra VB and Kim YK. Fracture and impact characterization of novel auxetic Kevlar®/Epoxy laminated composites. *Composite Structures* 2017; 168: 120-129.
19. Wang Z and Hu H. Tensile and forming properties of auxetic warp-knitted spacer fabrics. *Textile research journal* 2017; 87: 1925-1937.
20. Toronjo A. Articles of apparel including auxetic materials. Google Patents, 2017.
21. Zhang N, Chen J, Huang Y, et al. A wearable all-solid photovoltaic textile. *Advanced Materials* 2016; 28: 263-269.
22. Chen J, Huang Y, Zhang N, et al. Micro-cable structured textile for simultaneously harvesting solar and mechanical energy. *Nature Energy* 2016; 1: 16138.
23. Lin Z, Yang J, Li X, et al. Large-scale and washable smart textiles based on triboelectric nanogenerator arrays for self-powered sleeping monitoring. *Advanced Functional Materials* 2018; 28: 1704112.
24. Meng K, Chen J, Li X, et al. Flexible weaving constructed self-powered pressure sensor enabling continuous diagnosis of cardiovascular disease and measurement of cuffless blood pressure. *Advanced Functional Materials* 2019; 29: 1806388.
25. Hou T-C, Yang Y, Zhang H, et al. Triboelectric nanogenerator built inside shoe insole for harvesting walking energy. *Nano Energy* 2013; 2: 856-862.
26. Meng K, Zhao S, Zhou Y, et al. A Wireless Textile-Based Sensor System for Self-Powered Personalized Health Care. *Matter* 2020; 2 (4): 896-907.

27. Wright JR, Burns MK, James E, et al. On the design and characterisation of low-stiffness auxetic yarns and fabrics. *Textile Research Journal* 2012; 82: 645-654.
28. Grimmelsmann N, Meissner H and Ehrmann A. 3D printed auxetic forms on knitted fabrics for adjustable permeability and mechanical properties. In: *IOP Conference Series: Materials Science and Engineering* 2016, p.012011. IOP Publishing.
29. Zhou L, Jiang L and Hu H. Auxetic composites made of 3D textile structure and polyurethane foam. *physica status solidi (b)* 2016; 253: 1331-1341.
30. Steffens F, Rana S and Fangueiro R. Development of novel auxetic textile structures using high performance fibres. *Materials & Design* 2016; 106: 81-89.
31. Duncan O, Shepherd T, Moroney C, et al. Review of auxetic materials for sports applications: Expanding options in comfort and protection. *Applied Sciences* 2018; 8: 941.
32. Wang Z and Hu H. Auxetic materials and their potential applications in textiles. *Textile Research Journal* 2014; 84: 1600-1611.
33. Alderson K, Alderson A, Smart G, et al. Auxetic polypropylene fibres: Part 1-Manufacture and characterisation. *Plastics, Rubber and Composites* 2002; 31: 344-349.
34. Mizzi L, Azzopardi KM, Attard D, et al. Auxetic metamaterials exhibiting giant negative Poisson's ratios. *physica status solidi (RRL)–Rapid Research Letters* 2015; 9: 425-430.
35. Hu H and Zulifqar A. Auxetic textile materials-a review. *J Textile Eng Fashion Technol* 2016; 1: 00002.
36. Ren X, Das R, Tran P, et al. Auxetic metamaterials and structures: a review. *Smart materials and structures* 2018; 27: 023001.
37. Zhang G, Ghita OR and Evans KE. Dynamic thermo-mechanical and impact properties of helical auxetic yarns. *Composites Part B: Engineering* 2016; 99: 494-505.
38. Ng W and Hu H. Woven fabrics made of auxetic plied yarns. *Polymers* 2018; 10: 226.
39. Zhao S, Hu H, Kamrul H, et al. Development of auxetic warp knitted fabrics based on reentrant geometry. *Textile Research Journal* 2019: 0040517519866931.
40. Ma P, Chang Y and Jiang G. Design and fabrication of auxetic warp-knitted structures with a rotational hexagonal loop. *Textile Research Journal* 2016; 86: 2151-2157.
41. Alderson K, Alderson A, Anand S, et al. Auxetic warp knit textile structures. *physica status solidi (b)* 2012; 249: 1322-1329.
42. Zulifqar, A., Hua, T. and Hu, H., Single and Double Layered Bi-Stretch Auxetic Woven Fabrics Made of Non-Auxetic Yarns Based on Foldable Geometries. *physica status solidi (b)*2019: 10.1002/pssb.201900156.
43. Zulifqar A and Hu H. Development of bi-stretch auxetic woven fabrics based on re-entrant hexagonal geometry. *physica status solidi (b)* 2019; 256: 1800172.
44. Yang W, Li Z-M, Shi W, et al. Review on auxetic materials. *Journal of materials science* 2004; 39: 3269-3279.